Electronic Supplementary Material (ESI) for Analyst.


---

**SUPPORTING INFORMATION**

# Specification of Nitrogen Functional Group in Hydrotreated Petroleum Molecule by Hydrogen/Deuterium Exchange Electrospray Ionization High-Resolution Mass Spectrometry

Ying Zhang, Xiu Chen, Linzhou Zhang*, Quan Shi, Suoqi Zhao, Chunming Xu

*State Key Laboratory of Heavy Oil Processing & Petroleum Molecular Engineering Center (PMEC), China University of Petroleum, Beijing 102249, People's Republic of China*

*Corresponding Author Email: lzz@cup.edu.cn (L. Zhang);

*Table S1.* Model compounds information.

| No. | Name | Structure | Formula | Exact mass | Purchased From |
|---|---|---|---|---|---|
| 1 | Quinoline |  | $C_9H_7N_1$ | 129.05785 | Sigma-Aldrich |
| 2 | 5,6,7,8-tetrahydroquinoline |  | $C_9H_{11}N_1$ | 133.08915 | Aladdin |
| 3 | 4-phenylpyridine | 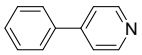 | $C_{11}H_9N_1$ | 155.07350 | Aladdin |
| 4 | Decahydroquinoline |  | $C_9H_{17}N_1$ | 139.13610 | Aladdin |
| 5 | 1,2,3,4-tetrahydroquinoline |  | $C_9H_{11}N_1$ | 133.08915 | Aladdin |
| 6 | Indoline |  | $C_8H_9N_1$ | 119.07350 | Aladdin |
| 7 | 1-(naphthalen-2-yl) ethan-1-amine | 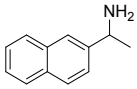 | $C_{12}H_{13}N_1$ | 171.10480 | Aladdin |
| 8 | 2-propylaniline | 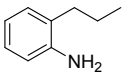 | $C_9H_{13}N_1$ | 135.10480 | TCI |

Table S2. Elemental analysis of CGO and VR

| Elemental Composition | CGO | Heavy Oil | | | | | | |
|---|---|---|---|---|---|---|---|---|
| | HT Product | VR Ⅰ | | VR Ⅱ | | | | |
| | | Feedstock | HT Product | Feedstock | VR Ⅱ-R1 | VR Ⅱ-R2 | VR Ⅱ-R3 | VR Ⅱ-R4 |
| C, wt% | 85.37 | 86.40 | 85.57 | 87.03 | 86.78 | 87.03 | 86.91 | 86.81 |
| H, wt% | 13.15 | 12.76 | 13.22 | 11.36 | 11.49 | 11.57 | 11.87 | 12.34 |
| O, wt% | 1.41 | 1.03 | 0.86 | 1.07 | 1.14 | 0.84 | 0.80 | 0.58 |
| N, ppm | 709 | 3200 | 2700 | 5272 | 5813 | 5468 | 4159 | 2693 |
| S, ppm | 17 | 5100 | 1000 | 19262 | 14030 | 6064 | 2278 | 1396 |

Table S3. Relative abundance of model compounds dissolved in DT-DM, DT-DM+$D_2O$, DT-DM+DCOOD, DT-DM+DCOOD+$D_2O$.

| No. | Class | Compounds | DM-DT Relative Abundance (%) | | | | DM-DT+$D_2O$ Relative Abundance (%) | | | | DM-DT+DCOOD Relative Abundance (%) | | | | DM-DT+$D_2O$+DCOOD Relative Abundance (%) | | | |
|---|---|---|---|---|---|---|---|---|---|---|---|---|---|---|---|---|---|---|
| | | | $d_0H^+$ | $d_0D^+$ | $d_1D^+$ | $d_2D^+$ | $d_0H^+$ | $d_0D^+$ | $d_1D^+$ | $d_2D^+$ | $d_0H^+$ | $d_0D^+$ | $d_1D^+$ | $d_2D^+$ | $d_0H^+$ | $d_0D^+$ | $d_1D^+$ | $d_2D^+$ |
| 1 | Pyridine | Quinoline | 30.00 | 100 | | | 23.14 | 100 | | | 24.15 | 100 | | | 8.26 | 100 | | |
| 2 | | 5,6,7,8-tetrahydroquinoline | 30.14 | 100 | | | 22.09 | 100 | | | 23.84 | 100 | | | 9.07 | 100 | | |
| 3 | | 4-phenylpyridine | 33.35 | 100 | | | 23.79 | 100 | | | 26.77 | 100 | | | 10.48 | 100 | | |
| 4 | Non-aromatic cyclic amine | Decahydroquinoline | 1.03 | 14.68 | 100 | | 0.66 | 11.89 | 100 | | 3.00 | 30.35 | 100 | | 0.59 | 14.57 | 100 | |
| 5 | cyclic aniline | 1,2,3,4-tetrahydroquinoline | 23.01 | 99.61 | 100 | | 5.95 | 60.00 | 100 | | 6.61 | 55.33 | 100 | | 0.32 | 10.88 | 100 | |
| 6 | | Indoline | 9.48 | 55.78 | 100 | | 2.68 | 24.80 | 100 | | 1.43 | 19.66 | 100 | | 0.51 | 9.10 | 100 | |
| 7 | non-aniline | 1-(naphthalen-2-yl)ethan-1-amine | 0.37 | 17.37 | 71.36 | 100 | 0.28 | 11.24 | 59.61 | 100 | 0.11 | 7.76 | 49.82 | 100 | 0.00 | 0.78 | 19.84 | 100 |
| 8 | aniline | 2-propylaniline | 2.60 | 44.08 | 100 | 94.38 | 1.31 | 11.79 | 51.18 | 100 | 0.67 | 8.95 | 44.57 | 100 | 0.00 | 0.81 | 11.90 | 100 |

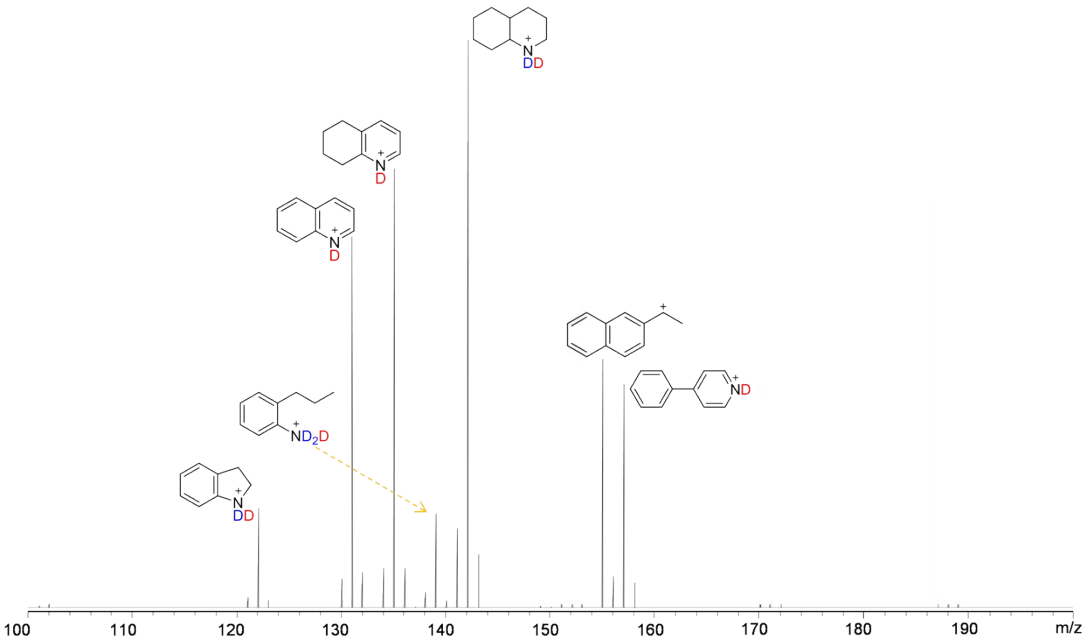


Figure S1. The (+) ESI Orbitrap mass spectra of mixed model compounds with the same molar mass. The aliphatic cyclic amine has higher relative abundance than others, but anilines have lower ionization efficiencies. Due to the easier fragmentation of the 1-(naphthalen-2-yl)ethan-1-amine's C-N bond, the relative abundance of N1H3 is extremely low, and the mainly expressed of the amine as $[M\text{-}NH_2]^+$.

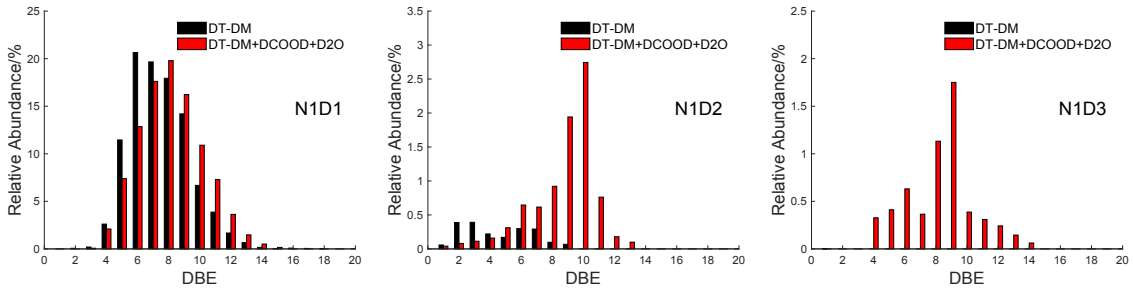


Figure S2. DBE distributions of (A) N1D1, (B)N1D2 and (C)N1D3 of the CGO dissolved in DT-DM or DT-DM+DCOOD+$D_2O$ detected by (+) ESI FT-ICR MS.

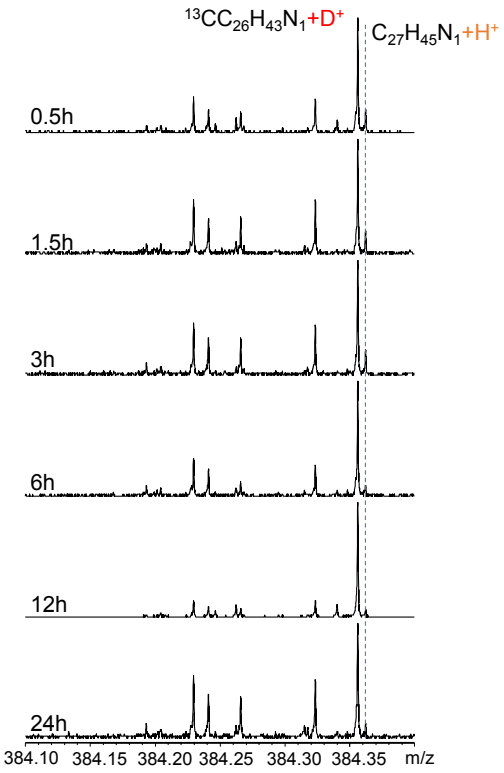


Figure S3. Expanded (+) ESI FT-ICR MS spectra for VGO dissolved in DT-DM with different HDX reaction time. Reaction time is 0.5 h, 1.5 h, 3 h, 6 h, 12 h or 24 h. Prolonging the reaction time can slightly reduce the relative abundance of N1H1.

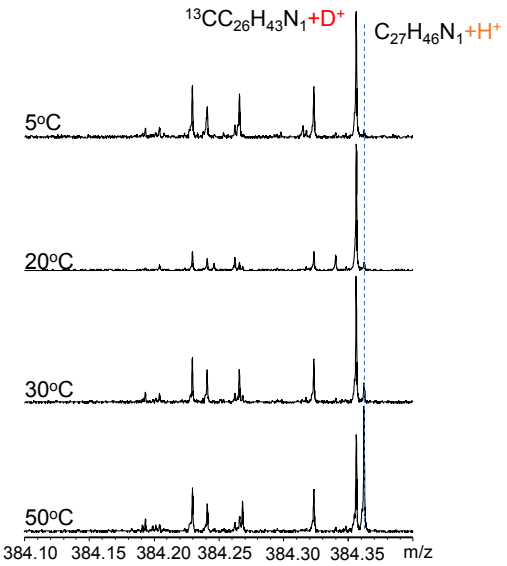


Figure S4. Expanded (+) ESI FT-ICR MS spectra and the relative abundance of N1H1 for crude oil's distillation cut dissolved in DT-DM with different reaction temperature. 5 °C means reacted in refrigerator at 5 °C for 30 minutes. 20 °C means reacted at room temperature for 30 minutes. 30 °C and 50 °C means reacted on hot plates of 30 °C and 50 °C for 30 minutes, respectively. The increase of the reaction temperature makes relative abundance of N1H1 increase significantly, but the relative abundance change of the N1H1 is negligible at room temperature and refrigeration conditions.

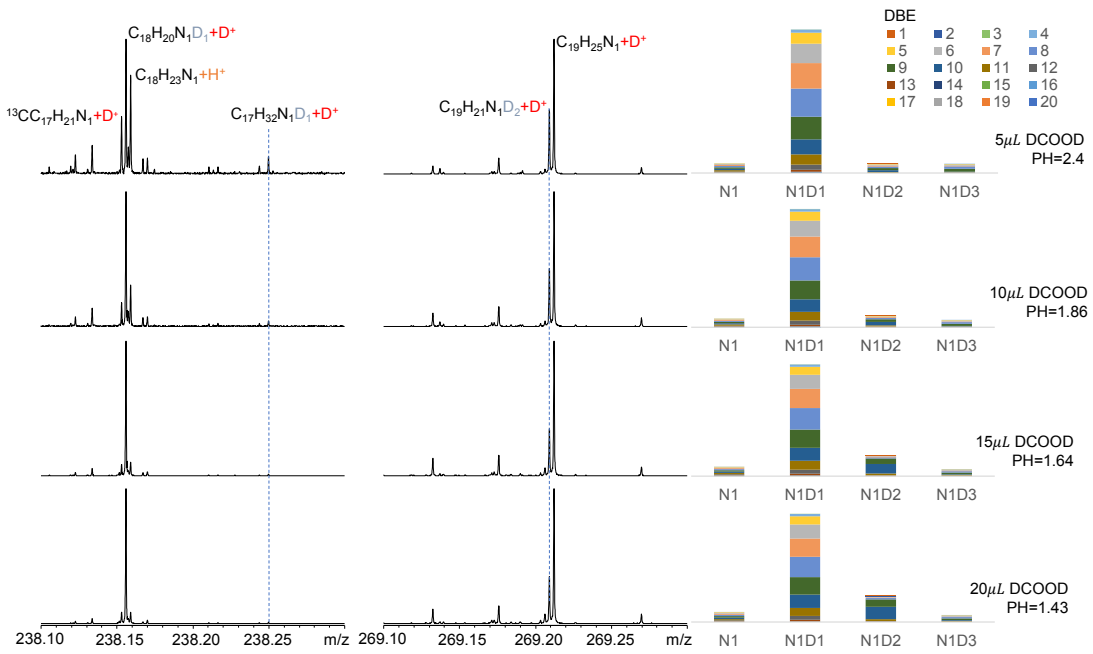


Figure S5. Expended mass spectra and the relative abundance distribution of N1 class species of the CGO dissolved in DT-DM+DCOOD+$D_2O$ with different DCOOD addition detected by (+) ESI FT-ICR MS. The increase of the DCOOD addition significantly increase the relative abundance of N1D2 class speices.

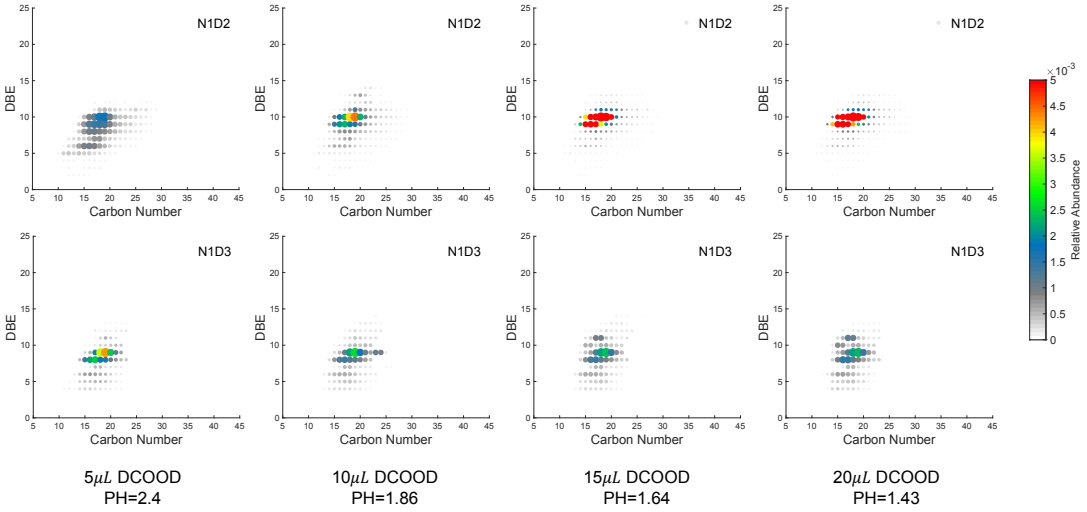


Figure S6. Plots of DBE versus carbon number for N1D2 and N1D3 classes species of the CGO dissolved in DT-DM+DCOOD+$D_2O$ with different DCOOD addition detected by (+) ESI FT-ICR MS.

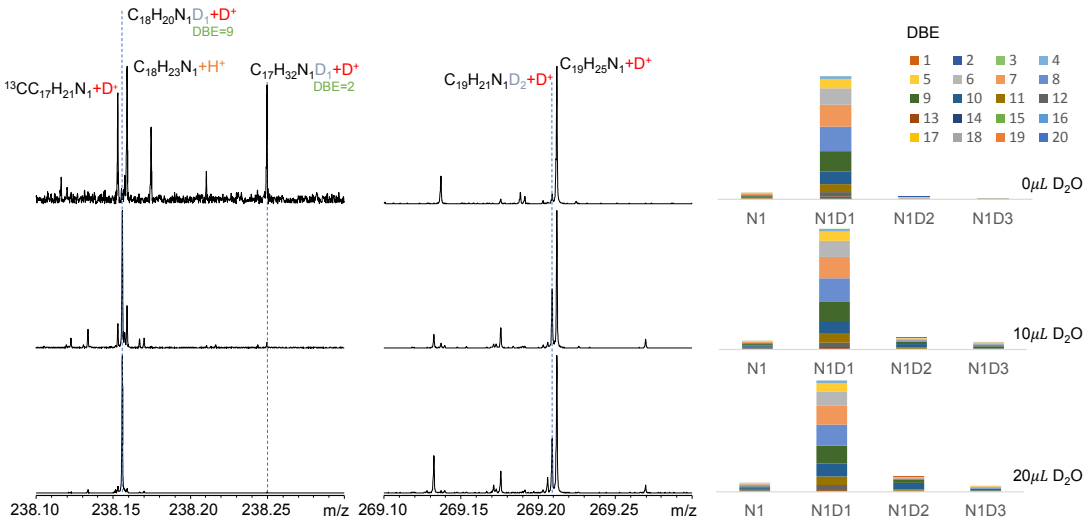


Figure S7. Expended mass spectra and the relative abundance distribution of N1 class species of the CGO dissolved in DT-DM+DCOOD+$D_2O$ with different $D_2O$ addition detected by (+) ESI FT-ICR MS. The increase of the $D_2O$ addition makes relative abundance of N1D2 and N1D3 increase significantly, but when the addition is 20 $\mu L$, the heavy oil solution will be opacified.

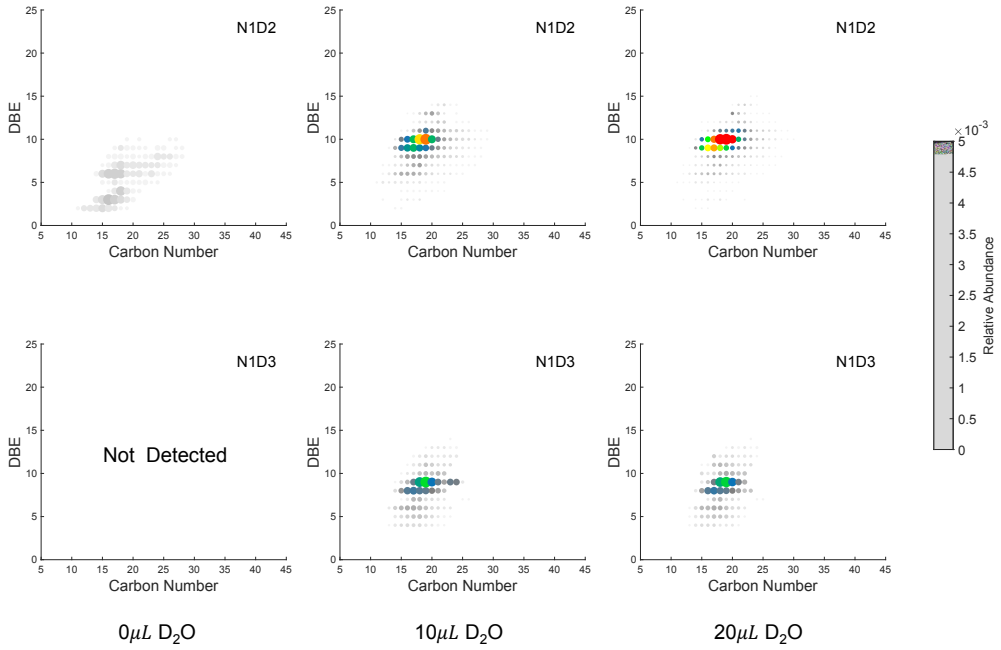


Figure S8. Plots of DBE versus carbon number for N1D2 and N1D3 classes species of the CGO dissolved in DT-DM+DCOOD+$D_2O$ with different $D_2O$ addition detected by (+) ESI FT-ICR MS. In order to detected more N1D2 and N1D3 peaks, the 10 $\mu L$ DCOOD and 10 $\mu L$ $D_2O$ were chosen to be added.

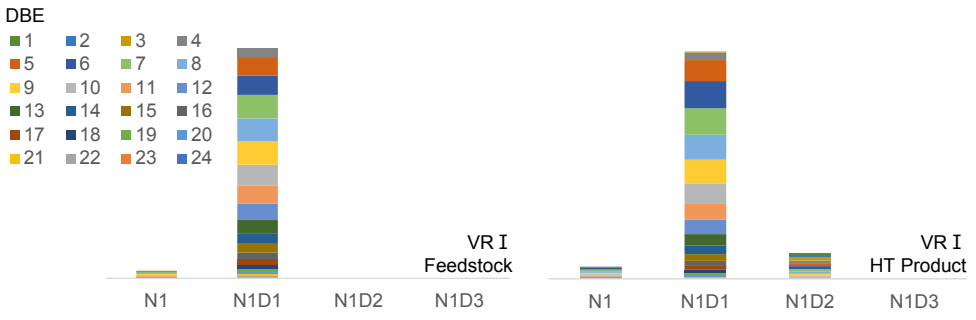


Figure S9. The relative abundance distribution of N1 class species of the VR Ⅰ before and after hydrotreating detected by HDX (+) ESI FT-ICR MS.

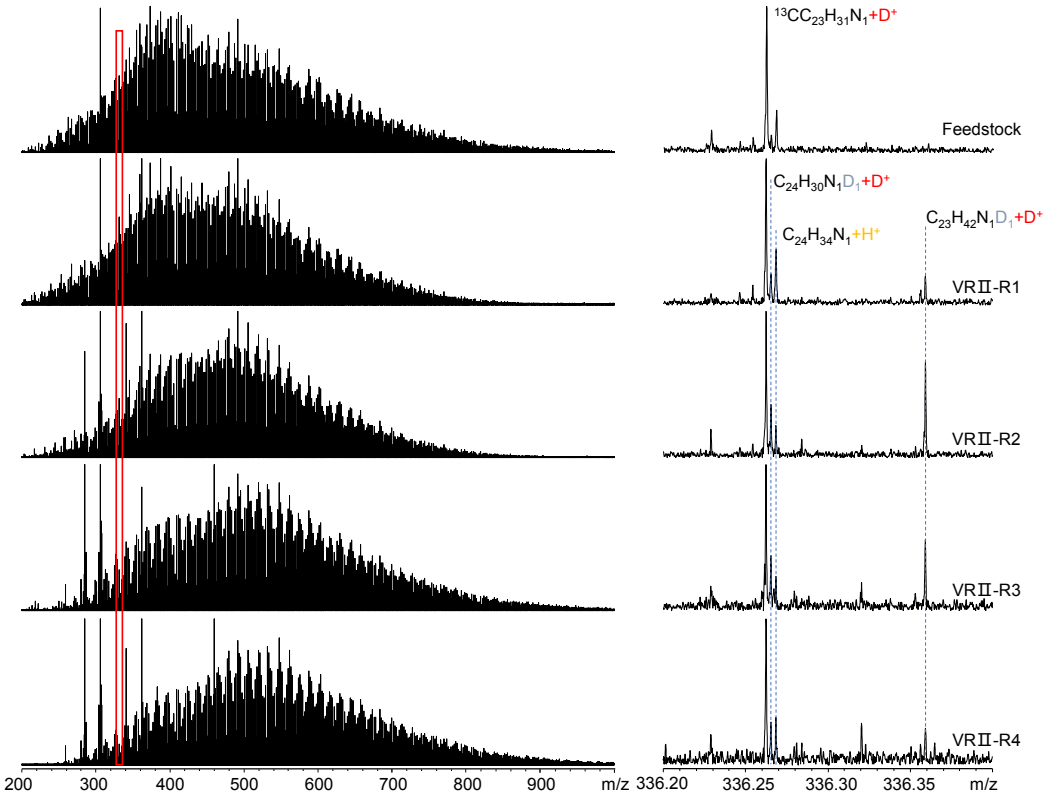


Figure S10. Broadband and expanded HDX (+) ESI FT-ICR MS spectra of the VR Ⅱ before and after hydrotreating.

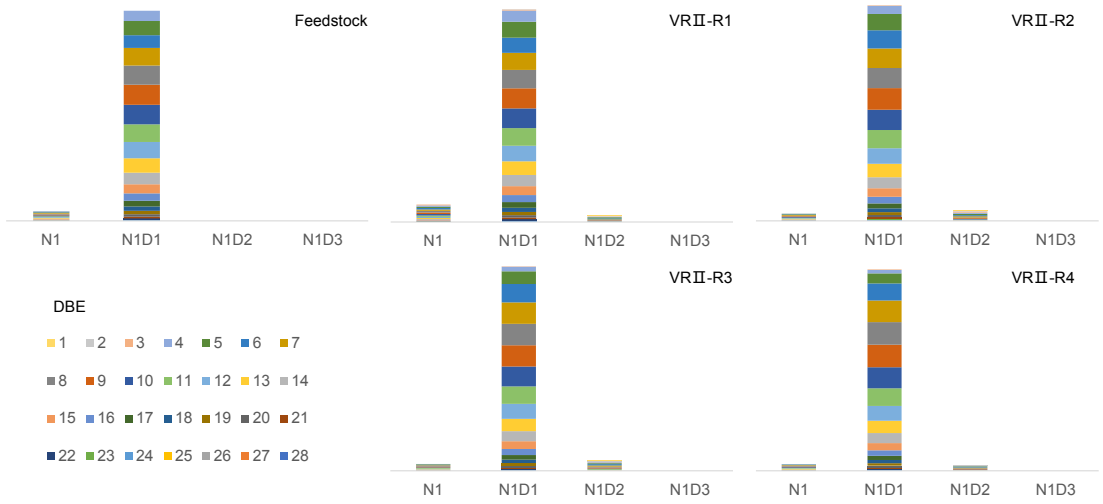


Figure S11. The relative abundance distribution of N1 class species of the VR Ⅱ before and after hydrotreating detected by HDX (+) ESI FT-ICR MS.